Research Article

Milad Torabfam and Meral Yüce*

Microwave-assisted green synthesis of silver nanoparticles using dried extracts of *Chlorella vulgaris* and antibacterial activity studies

https://doi.org/10.1515/gps-2020-0024
received November 14, 2019; accepted February 04, 2020

Abstract: Green synthesis of metallic nanoparticles (NPs) is acquiring considerable attention due to its environmental and economic superiorities over other methods. This study describes the practical synthesis of silver nanoparticles (AgNPs) through the reduction of silver nitrate solution using an algal source, *Chlorella vulgaris*, as the reducing as well as the stabilizing agent. The energy required for this synthesis was supplied by microwave radiation. The ultraviolet-visible spectroscopy exhibited a single peak related to the surface plasmon absorbance of AgNPs at 431 nm. The AgNPs with high stability (a zeta potential of −17 mV), hydrodynamic size distribution of 1–50 nm, and mostly spherical shape were obtained through a 10 min process. Fourier transform infrared spectroscopy analysis revealed that several functional groups, including carbonyl groups of *C. vulgaris*, play a significant role in the formation of functional NPs. Antibacterial features of the produced AgNPs were verified against those of *Salmonella enterica* subsp. *enterica serovar typhimurium* and *Staphylococcus aureus*, demonstrating a considerable growth inhibition at increasing concentrations of the NPs. As a result, the formed AgNPs can be used as a promising agent against bacterial diseases.

Keywords: green synthesis, microwave synthesis, silver nanoparticles, algae, *Chlorella vulgaris*, antimicrobial activity

1 Introduction

Nanoscience stands out among the futuristic fields of research. Within this field, the synthesis of workable metal nanoparticles (NPs) using biological procedures has attracted significant attention worldwide [1,2]. Metal NPs present striking physicochemical features when compared to individual molecules and macro metals as a result of high surface area to volume ratios [3]. In the case of silver nanoparticles (AgNPs), based on their sizes and shapes, their fundamental properties such as electrical and thermal conductivity, catalytic activity, solubility, and sensitivity enable widespread employment of them in food packaging, water treatment tasks, and drug delivery applications [4–6]. A variety of methods ranging from sonoelectrochemical methods and chemical reduction to ultraviolet (UV) irradiation can be implemented for the synthesis of AgNPs [7–9]. The fact that applying some of these synthesis methods results in purified AgNPs cannot be neglected. In contrast, however, the synthesis cost must be considered as a fundamental factor in a formation procedure. Furthermore, using hazardous chemical materials as agents during synthesis raises serious questions about environmental toxicity and safety issues in the fabrication process. Consequently, the request has been increasing for green methods, which are more secure, practical, and environmentally friendly than current physical and chemical methods [10]. The plants along with products of plants and microorganisms (e.g., algae, yeast, fungi, and bacteria) have been used as natural alternatives to other chemicals during synthesis leading to the formation of metal NPs. Compared with other conventional methods, NPs formed by biosynthesis contain non-toxic by-products that improve NP biocompatibility in various applications [11]. Being nature friendly [2], affordable [12], maintainable [13], and free from chemical pollution [14], biological agents have become excellent candidates for the production of NPs. Furthermore, the green synthesis of NPs using microorganisms has become the center of attention over the past few years due to remarkable properties, such as lower synthesis time [15], and it is a low-priced, safe, reliable [16], and single-step [14] procedure. Due to the

* **Corresponding author: Meral Yüce,** SUNUM Nanotechnology Research and Application Centre, Sabanci University, 34956, Istanbul, Turkey, e-mail: meralyuce@sabanciuniv.edu
Milad Torabfam: Faculty of Engineering and Natural Sciences, Sabanci University, 34956, Istanbul, Turkey

capping feature of components in microorganisms, addition of extra stabilizers is not required [11].

It is also known that metal NPs, as an alternative to antibiotics, exhibit outstanding antibacterial properties [15]. Besides this, their antifungal activity is considerable [17]. Among several noble metal NPs, AgNPs have been reported to have the most impressive antimicrobial features against various kinds of microorganisms, as summarized in Table 1. Being capable of stabilizing AgNPs, proteins and sugars of biological molecules used as reducing and stabilizing agents during synthesis are salient biotic components contributing to NP interactions with other organisms as well as microorganisms, which results in enhanced antimicrobial properties of the formed NPs. By making contact with the cell membrane and without penetrating it, AgNPs can apply the antibacterial effect and cause the death of microorganisms [18,19]. In the case of the energy needed for the synthesis, although numerous well-established techniques are available, the synthesis method must contain simplified and cost-effective procedures and be capable of increasing the reaction rate by orders of magnitude. Moreover, short reaction periods and higher efficiency to produce pure NPs are significant factors to be considered while choosing a method to synthesize NPs. Fulfilling the abovementioned criteria, microwave irradiation as a desirable and primary heating method surpasses conventional heating methods [20,21]. In 2,000, the required energy for the synthesis of $PbTiO_3$ NPs using ethylene glycol as a reducing agent was provided by microwave. This new method of supplying energy was investigated by Palchik et al. [22]. Due to striking features, including being fast, straightforward, and energy-saving, the Palchik group made use of this method for the acceleration and stabilization of the reactions. The average diameter of the NPs obtained through this method was around 15 nm, and only 1 min of microwave heating was applied in order to supply the energy required for the reaction. The microwave-assisted synthesis method produces NPs with lower dispersion, which is arranged in a more regular pattern. It is noteworthy that the shape and morphology of the formed nanostructures can be controlled in this procedure [20].

With a history of approximately 3.4 billion years, microalgae possess a distinct characteristic of high biodiversity. Among various microalgae, eukaryotic green microalgae *Chlorella vulgaris* from genus *Chlorella* has been present on earth since the Precambrian era [23]. *C. vulgaris* is a ball-shaped atomic type of cell with a diameter ranging from 2 to 10 μm and contains numerous constituents, including cell wall and cytoplasm with mitochondrion and chloroplast organelles. The primary components of *C. vulgaris* are proteins, lipids, carbohydrates, pigments, minerals, and vitamins. Proteins are incredibly significant in the algal structure and constitute half of the dry weight of the fully grown *C. vulgaris* cell. Besides proteins, lipids are made up of various ingredients, such as glycolipids and hydrocarbons. Carbohydrates such as starch and cellulose are examples of polysaccharides that existed in *C. vulgaris* [23,24]. Also, polysaccharides extracted from algae have a dual impact due to their ability to reduce silver ions and stabilize the formed AgNPs [25]. Figure 1 summarizes the main methods of synthesis along with subdivisions of green synthesis. The schematic illustration of AgNPs in this report is also presented.

In this study, the dried-biomass of *C. vulgaris* algae was used for the first time in the microwave-assisted green synthesis of AgNPs. As presented in Table 1, only a few studies have been conducted so far with algae for NP synthesis, and only a limited number of tests regarding antibacterial activity have been investigated. Here, we also report the antibacterial activity of the formed AgNPs against the well-known foodborne pathogens, including *Salmonella enterica* subsp. *enterica serovar typhimurium* (Gram−) and *Staphylococcus aureus* (Gram+).

2 Materials and methods

2.1 Materials

Silver nitrate ($AgNO_3$) with a purity of 99.9% as a silver ion precursor was provided by Merck (Germany). Foodborne pathogens, *Salmonella enterica* subsp. *enterica serovar typhimurium* (ATCC® 14028™) and *S. aureus* (ATCC® 29213™), were acquired from American Type Culture Collection (ATCC, USA). Nutrient agar (NA) and nutrient broth (NB) as a cultivation medium were bought from Oxoid Ltd (Hampshire, England). Deionized double distilled water was used to prepare the required solutions.

2.2 Algae preparation

The cultivation of microorganisms in the BG11 medium was done by the flask-shake method [46]. *C. vulgaris* cells were collected through centrifugation at 10,000 rpm for 15 min. Then, the supernatant was separated, and the pellet was cleaned using sterile water. The glass plates were used for heat drying of algal biomass at 55°C for 24 h.

Table 1: Green synthesis of AgNPs using plants and microorganisms.

Reducing or stabilizing agent	Size (nm)	Antimicrobial activity	Reference
Turmeric powder	18 ± 0.5	*Escherichia coli*, *Listeria monocytogenes*	[26]
Thymbra spicata	7	NA	[27]
Calliandra haematocephala leaf	70	*E. coli*	[28]
Gracilaria birdiae	20.2–94.9	*E. coli*, *Staphylococcus aureus*	[29]
Crocus sativus L.	12–20	*E. coli*, *Pseudomonas aeruginosa*, *Klebsiella pneumoniae*, *Shigella flexneri*, *Bacillus subtilis*	[30]
Rheum palmatum root	121 ± 2	*S. aureus*, *P. aeruginosa*	[31]
Alysicarpus monilifer leaf	15 ± 2	MRSA and CoNS	[32]
Elephantopus scaber	37.86	*B. subtilis*, *Lactococcus lactis*, *Pseudomonas fluorescens*, *P. aeruginosa*, *Aspergillus flavus*, *Aspergillus penicillioides*	[33]
Eriobotrya japonica	20	*E. coli*, *S. aureus*	[34]
Cladosporium cladosporioides (fungi)	<100	*E. coli*, *S. aureus*, *B. subtilis*, *Staphylococcus epidermis*, *Candida albicans*	[1]
Botryosphaeria rhodina (fungi)	2–50	NA	[35]
Ganoderma sessiliforme (fungi)	45.26	*E. coli*, *B. subtilis*, *Streptococcus faecalis*, *Listeria innocua*, *Micrococcus luteus*	[16]
Padina pavonica (algae)	49.58–86.37	NA	[10]
Bacillus amyloliquefaciens, *B. subtilis* (bacteria)	<100	*S. aureus*, *E. coli*, *P. aeruginosa*, *Streptococcus pyogenes*, *C. albicans*	[36]
Gelidium amansii (algae)	27–54	*S. aureus*, *Bacillus pumilus*, *E. coli*, *P. aeruginosa*, *Vibrio parahaemolyticus*, *Aeromonas hydrophila*	[2]
Bacillus brevis (bacteria)	41–68	*Salmonella typhi*, *S. aureus*	[4]
Laminaria japonica (algae)	20–31	NA	[14]
Streptomyces species (bacteria)	8.4	*B. subtilis*, *S. aureus*, *K. pneumoniae*, *P. aeruginosa*, *E. coli*, *Proteus mirabilis*, *Salmonella infantis*	[37]
Rhizopus stolonifer (fungi)	9.46 ± 2.64	NA	[38]
Enteromorpha compressa (algae)	4–24	*E. coli*, *K. pneumoniae*, *P. aeruginosa*, *S. aureus*, *Salmonella paratyphoid*, *Aspergillus niger*, *A. flavus*, *Aspergillus ochraceus*, *Fusarium moniliforme*, *Aspergillus terreus*	[6]
Duddingtonia flagrans (fungi)	11–38	NA	[13]
Pleurotus ostreatus (fungi)	<40	*B. subtilis*, *Bacillus cereus*, *S. aureus*, *E. coli*, *P. aeruginosa*	[12]
Bacillus methylotrophicus (bacteria)	10–30	*C. albicans*, *Salmonella enterica*, *E. coli*, *V. parahaemolyticus*, *C. albicans*	[39]
Pseudomonas deceptionensis (bacteria)	10–30	*S. aureus*, *S. enterica*, *V. parahaemolyticus*, *C. albicans*, *Bacillus anthracis*	[40]
Weissella oryzae (bacteria)	10–30	*V. parahaemolyticus*, *B. cereus*, *B. anthracis*, *S. aureus*, *E. coli*, *C. albicans*	[41]
Arthroderma fulvum (fungi)	15.5 ± 2.5	*C. albicans*, *Candida parapsilosis*, *Candida krusei*, *Candida tropicalis*, *Aspergillus fumigatus*, *A. flavus*, *Aspergillus terreus*, *Fusarium solani*, *F. moniliforme*, *Fusarium oxysporum*	[42]
Bhargavaea indica (bacteria)	30–100	*V. parahaemolyticus*, *S. enterica*, *S. aureus*, *B. anthracis*, *B. cereus*, *E. coli*, *C. albicans*	[43]
B. pumilus, *Bacillus persicus*, and *Bacillus licheniformis* (bacteria)	77–92	*E. coli*, *Shigella sonnei*, *P. aeruginosa*, *K. pneumoniae*, *Streptococcus bovis*, *Staphylococcus epidermidis*, *S. aureus*, *A. flavus*, *C. albicans*	[44]
L. monocytogenes, *B. subtilis*, *Streptomyces anulatus* (bacteria)	Various shapes and sizes	*Chrysosporium keratinophilum*	[45]
Candida utilis (fungi)	20–80	*P. aeruginosa S. aureus*, *E. coli*	[46]
Caulerpa racemosa (algae)	5–25	*S. aureus*, *P. mirabilis*	[47]
C. vulgaris (algae)	40–90	NA	[48]
C. vulgaris (algae)	24	*Salmonella enterica* subsp. *enterica serovar typhimurium*, *S. aureus*	This study

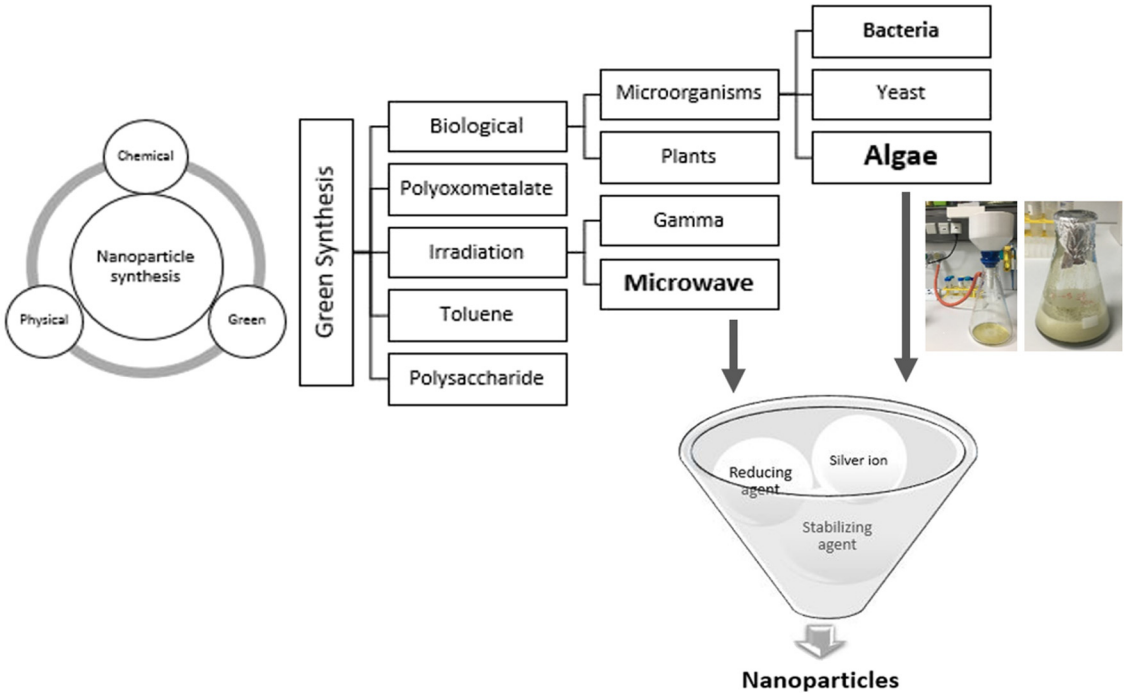

Figure 1: The main methods of NP synthesis as well as subdivisions of green synthesis along with a schematic demonstration of the current AgNP formation.

As a final step, dried biomass was removed from the plates and powdered using a mortar. The heat-dead biomass used in this assay can be handled and stored easily without any need for nutrient supply. Finally, biomass powder (1.6 g) was mixed with 100 mL of deionized water in an Erlenmeyer flask with a magnet inside it, kept on stirring at 50°C for 3 h and at 10°C for 21 h to be well dispersed. Then the solution was filtered using a filter paper and a vacuum filtration unit. The supernatant was kept in the fridge for further reaction and analysis.

2.3 NP synthesis

For the synthesis of AgNPs, 10 mL of *C. vulgaris* was mixed with 90 mL of an aqueous solution of $AgNO_3$ (1 mM solution) and heated by microwave at the power of 180 W for various time intervals. In order to take the sample from the solution during the heating process and prevent overheating, microwave radiation was applied for 2 min by 15 s delay for a total heating time of 10 min. The bioreduction of Ag^+ ions in the solution was checked by regular sampling (2 mL) of the suspension, then the UV-visible spectra of the taken sample were measured. The synthesis reaction was monitored by the UV-visible spectra, as well as by monitoring the color change in the reaction solution. Gradually, the original light-green color of the solution changed to red-brown color, indicating the formation of AgNPs. In all steps, the synthesized AgNPs were sonicated and filtered.

2.4 Characterization of NPs

The change in the color of the mixture containing the silver nitrate solution and *C. vulgaris* was monitored by visual observation. In order to confirm the formation of AgNPs, the reaction mixture was sampled at constant intervals of time. Following this, the absorption maximum (λ_{max}) was measured at 350–800 nm using a spectrophotometer (Cary 5000 UV-Vis-NIR, USA), which works based on surface plasmon resonance (SPR). In the aforementioned range, the excitation of surface plasmon vibration bands leads to a considerable alteration in the solution color. Due to the relationship between the absorbance of the produced AgNPs and their concentration, the synthesized AgNP concentration can be easily determined by UV-Vis spectroscopy in a 10 mm optical path quartz cuvette containing 1 mL of the target sample [18].

The Fourier transform infrared (FT-IR) analysis of AgNPs, including *C. vulgaris* and unmixed *C. vulgaris*,

was done to determine the functional groups of *C. vulgaris* and estimate their role as reducing or stabilizing agents in AgNP synthesis using an FT-IR spectrophotometer with a deuterated triglycine sulfate detector (Thermo Scientific Nicolet iS10, USA). The range used to record the FT-IR spectra was 4,000–400 cm^{-1}.

The mean hydrodynamic size of the synthesized AgNPs was evaluated using a dynamic light scattering (DLS) analyzer (Zetasizer Nano ZS, Malvern, UK) with a 10 mm optical path quartz cuvette containing 1 mL of the target sample. Brownian motion, as a principle used in this device, causes the scattered light intensity fluctuations, which are measured by the DLS analyzer [13]. This measurement leads to the determination of the number of particles as well as their hydrodynamic size in a solution. In the case of the size distribution of the particles, the NP polydispersity index (PDI), as a value varying from zero to one, can be computed using this device. In order to detect and calculate the surface charge of the synthesized AgNPs, their value of zeta potential, as a demonstration of their stability, can be provided at 25°C by the DLS analyzer [13].

Further insight into the morphology of the formed AgNPs, comprising size as well as shape, was provided using a scanning electron microscope (SEM) with a focused electron beam (Zeiss Leo Supra 35 VP, Germany) along with a transmission electron microscope (TEM; CM120, Philips, Amsterdam, The Netherlands) with an acceleration voltage of 120 kV. In order to provide a sample for both SEM and TEM analyses, 5 µL of the targeted solution was dropped on a silicon wafer and left to dry at room temperature for a couple of hours.

2.5 Antibacterial activity

Antibacterial effects of the green-synthesized NPs were tested using liquid and solid nutrient media on the agar plates. For each bacterium, the suspension provided by mixing 500 µL of NB with 50 µL of target bacterium was vortexed well as a first step, and five small test tubes were taken and 5 mL of NB was added in each tube. Then, 100 µL of the suspension containing NB and bacterium was added to each test tube. Following this, 30, 60, 90, and 300 µL of the formed AgNPs was added to second, third, fourth, and fifth tubes, respectively, to monitor the effect of AgNPs on bacterium growth. The AgNP solution was not added to the first tube, which was used as a control culture. Finally, all five tubes were incubated for 24 h at 37°C. Then, 200 µL of the bacterial suspensions prepared in each of the five tubes was inoculated into plates containing culture media of NA. Finally, the plates were placed in an incubator at 37°C for 24 h.

3 Results and discussion

3.1 Characterization of NP formation

As presented in Figure 2, the specific color change in the solution containing silver nitrate and *C. vulgaris* from pale green to reddish brown was the initial demonstration of the AgNP formation, and this color change is because of the excitation of vibration bands related to SPR [6]. The synthesis of AgNPs was verified by broad absorption peaks (λ_{max}) at wavelengths ranging from 380 to 450 nm. Owing to the SPR of AgNPs, the bands outlined above are ordinary absorption bands of these NPs. Noteworthy is the fact that the absorption of AgNPs was also reported between 410 and 440 nm in other research studies [2,16]. Figure 3 reveals that λ_{max} of the synthesized AgNPs was obtained at 431 nm with a concentration of 59.22 ppm, an indication of the successfully formed AgNPs, which was in the desirable range for AgNPs. In the first 4 min, no peak was noticed, confirming that no target product was formed. After 6 min of being exposed to microwave irradiation, the SPR band for NPs was obtained. A consistent growth was noticed in the intensity of synthesis with an increase in irradiation time without any considerable change in the peak position. Thus, the synthesized NP with higher intensity was achieved at 10 min. It is worth mentioning that the irradiation time of more than 10 min led to the evaporation of all remaining solutions. Furthermore, the results in Figure S1 show the repeatability of the method applied in this report.

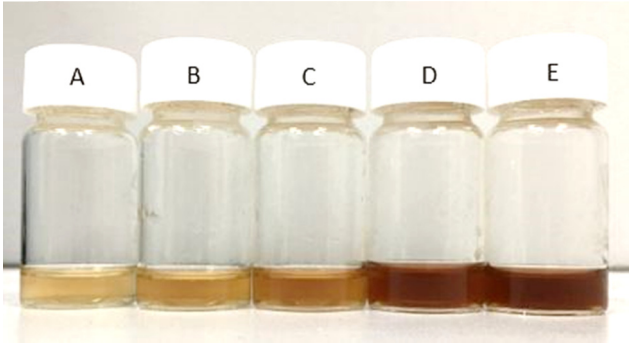

Figure 2: Various stages of AgNP formation after 2 (A), 4 (B), 6 (C), 8 (D), and 10 (E) min of microwave radiation.

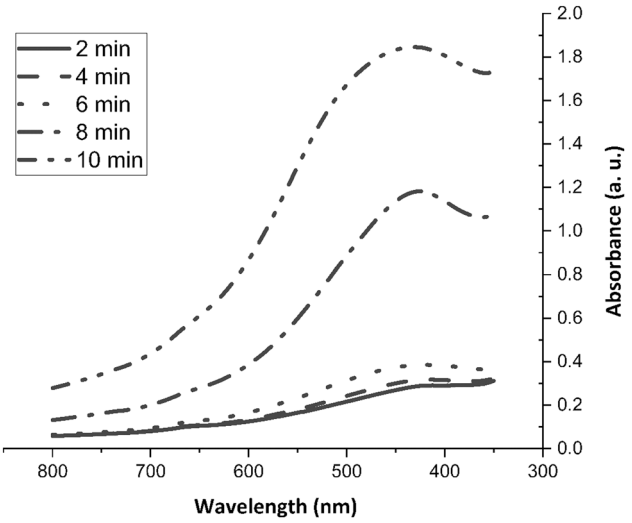

Figure 3: Recorded UV-Vis spectra of the provided AgNPs according to the microwave exposure time.

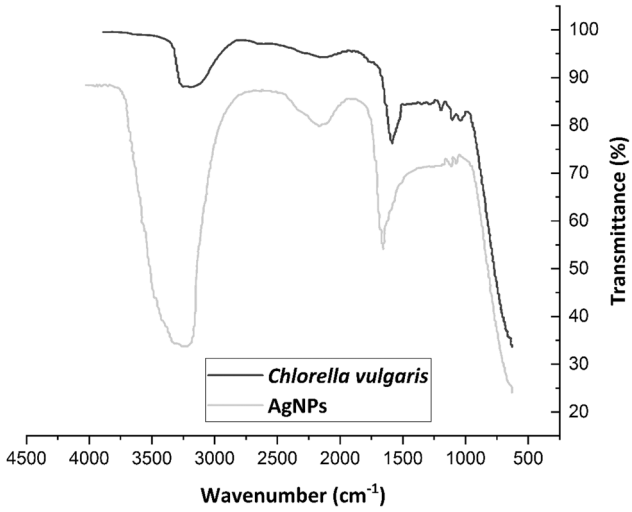

Figure 4: FT-IR spectra of *C. vulgaris* and prepared AgNPs.

The FT-IR spectra related to unmixed algae, as well as AgNP solutions, were analyzed to determine the various functional groups related to *C. vulgaris*, which are responsible for the reduction of the Ag^+. Furthermore, the intensity of several regions can be noticed using this spectrum. As evidently noted in Figure 4, two sharp absorption peaks exist at 3262.98 and 1635 cm^{-1}. The peak with the shape of U at around 3,200–3,300 cm^{-1} contains both O–H hydroxyl and N–H amine groups. Moreover, a broad peak between 1,621 and 1,645 cm^{-1} is related to the amide I band due to the carbonyl bond. A weak peak at around 2151.54 cm^{-1} corresponds to the N–C compounds. Also, the $-NH_2$ bond of the protein or polysaccharide in *C. vulgaris* appears as a peak at the wavelength of 1,155 cm^{-1}. Following this, the absorption bands at 1,081 cm^{-1} and 1,036 cm^{-1} can be attributed to the ν(C–O–C) bond of polysaccharides that existed in *C. vulgaris*. Between 1,036 and 3262.98 cm^{-1}, the abovementioned peaks can also be noticed in the infrared band of *C. vulgaris*, including NPs. A considerable shift in some of these peaks indicates the possible involvement of the carbonyl group and peptides of proteins related to algae in the synthesis of target NPs. *C. vulgaris* is rich in proteins and carbohydrates, providing a group of polysaccharides, which are of great importance in the composition of this alga. The results obtained are consistent with those of the study by Duygu et al. [49]. The FT-IR spectrum of *C. vulgaris*, obtained by their group, was a confirmation for the presence of proteins, groups of carbonyls, as well as polysaccharides involved in the reduction of Ag^+ along with stabilization of AgNPs.

Figures 5 and 6 shows the mean hydrodynamic size, PDI, and zeta potential of the formed NPs, which are 24.79 nm, 0.252, and –17 mV, respectively. With regard to the hydrodynamic size distribution pattern, particles with a size smaller than 100 nm are more noticeable after applying 2 min of microwave irradiation and increasing the

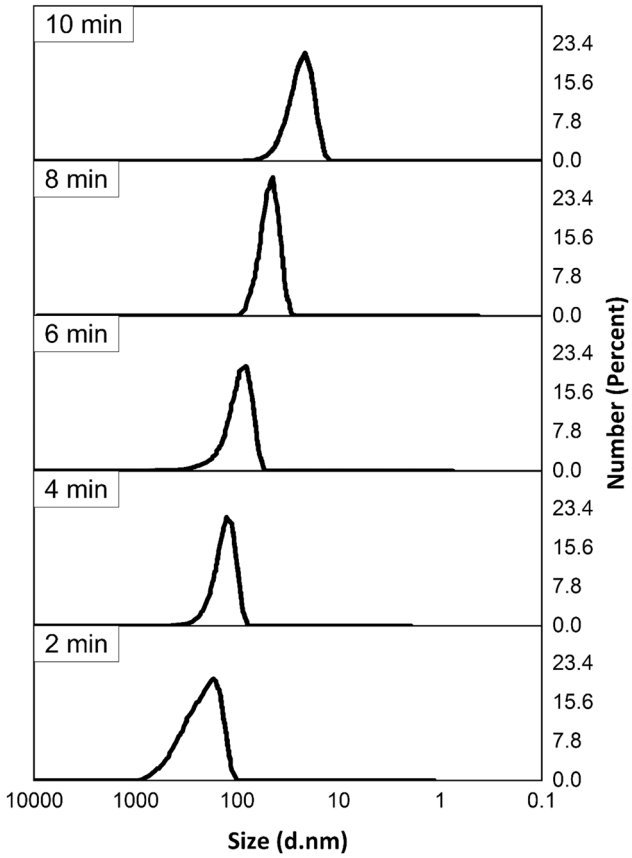

Figure 5: The hydrodynamic size distribution of the synthesized AgNPs after 2, 4, 6, 8, and 10 min of being exposed to microwave radiation.

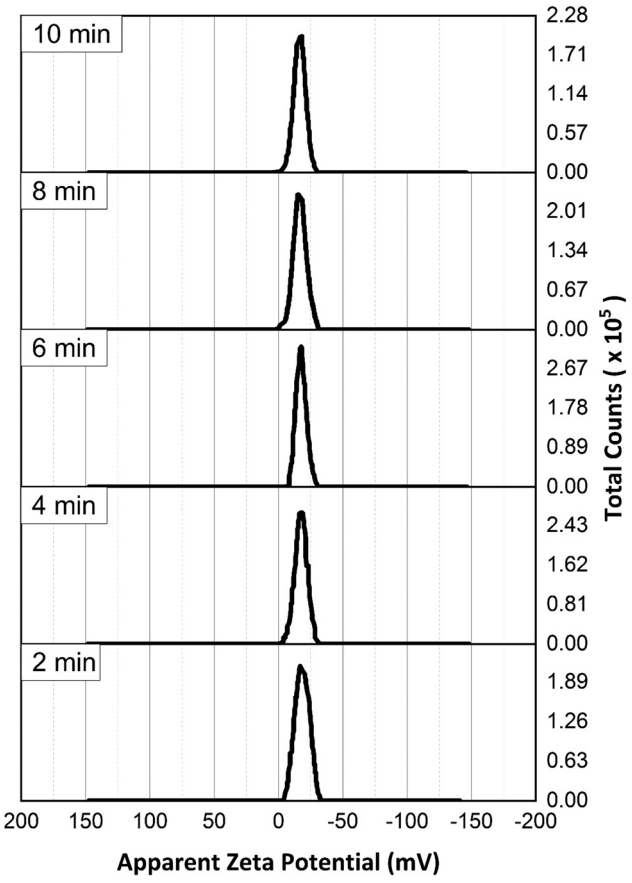

Figure 6: Zeta potential of the synthesized AgNPs after 2, 4, 6, 8, and 10 min exposure to microwave radiation.

microwave exposure time up to 10 min results in NPs with smaller hydrodynamic size. Finally, particles in the interval of 10–40 nm are obtained after 10 min of exposure to microwave irradiation (Figure 5). The AgNPs with lower PDI are more acceptable, and the PDI value of 0.252 in the current assay indicates the excellent distribution of particles in the target solution. A zeta potential of –17 mV, as an indicator of the electrical cloud around the NPs, reveals the high stability of the synthesized NPs. Due to the electric repulsion between particles, higher surface charge results in more stable suspension. It is worth mentioning that by periodic sampling of the suspension during 10 min of microwave exposure, the zeta potential values of the particles after 2, 4, 6, 8, and 10 min were measured and provided in Figure 6. The value of zeta potential related to the formed NPs was somewhere in the vicinity of –17 mV during this 10 min of reaction time. The results reported in this experiment are consistent with those of the previous experiments of Składanowski et al. and Elbeshehy et al. [37,44]. Składanowski and coworkers found the zeta potential of the formed AgNPs using *Streptomyces* sp. to be –19.4 mV. In the assay carried out by Elbeshehy et al., AgNPs formed by *Bacillus* spp. had a zeta potential of –18.5 mV. As shown in Figure S2, the reported method is repeatable, and AgNPs with a size smaller than 50 nm and a zeta potential of approximately –18 mV can be synthesized using this method.

As represented in Figures 7 and 8, TEM and SEM analyses clarify the size as well as the morphology of the

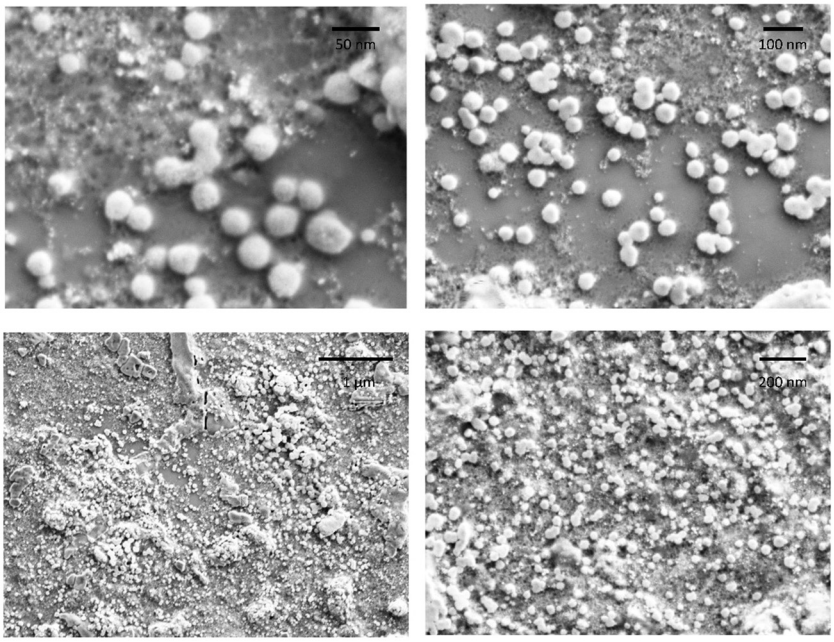

Figure 7: SEM images related to the produced AgNPs in various scale bars.

synthesized NPs. Figures 7 and 8, respectively, indicate that most of the AgNPs synthesized by *C. vulgaris* are spherical and quasi-spherical with flat edges. Following this, NPs with allotropic structures that have asymmetrical curves can be detected. Also, some of them are rectangular spheres, decahedral, and polygonal in shape. Being well dispersed with no aggregation, AgNPs have a size between 1 and 50 nm with an average size of 24.79 nm. Noteworthy is the fact that the difference in the size distribution of NPs can be related to the contribution of various molecules and functional groups to the reduction of silver ions and stabilization of AgNPs [12]. The formed AgNPs are surrounded by a thin capping layer of material obtained from the aqueous extract of *C. vulgaris*, which can be spotted by these images. The capping agent substantially prevents the Ag NP aggregation and consequently leads to the formation of NPs with higher stability [27]. The shape of particles has a significant role to play in the stability of NPs, and spherical NPs are highly stable in comparison with other shapes of NPs [18]. Also, a zeta potential value of –17 mV of the formed NPs is an excellent demonstration of high stability of particles in the nanoscale.

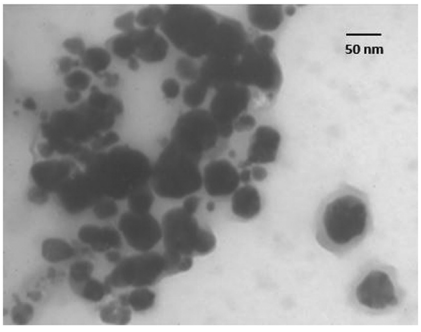

Figure 8: TEM images related to the produced AgNPs.

3.2 Antibacterial activity of the formed AgNPs

The antibacterial effect of AgNPs on *S. typhimurium*, as well as *S. aureus* bacteria, as a function of the volume of the synthesized AgNPs, is shown in Figure 9. As revealed in this figure, increasing the volume of the AgNP solution has a considerable detrimental effect on the bacterial growth rate for both bacteria. In the case of *S. aureus*, decrease in the number of colonies in the second, third, and fourth plates can be noticed, and the fifth tube (A5) is empty without any bacteria. In the case of *S. typhimurium*, the formed AgNPs have a more substantial antibacterial effect on this bacterium (Gram–) in comparison with the first one (Gram+) and the plates empty without any bacterium are shown in B3–B5 in Figure 9. The free positive ions of NPs stick to the negatively charged cell walls of both types of bacteria and apply their antibacterial effect on them. Studies in the past few years also confirmed higher resistance of Gram-positive bacteria against AgNPs in comparison with Gram-negative bacteria [50], which can be justified by the difference in the structure of the cell walls. Being covered by a layer of lipopolysaccharides and peptidoglycans, the cell of Gram-negative *S. typhimurium* is more susceptible to the entrance of

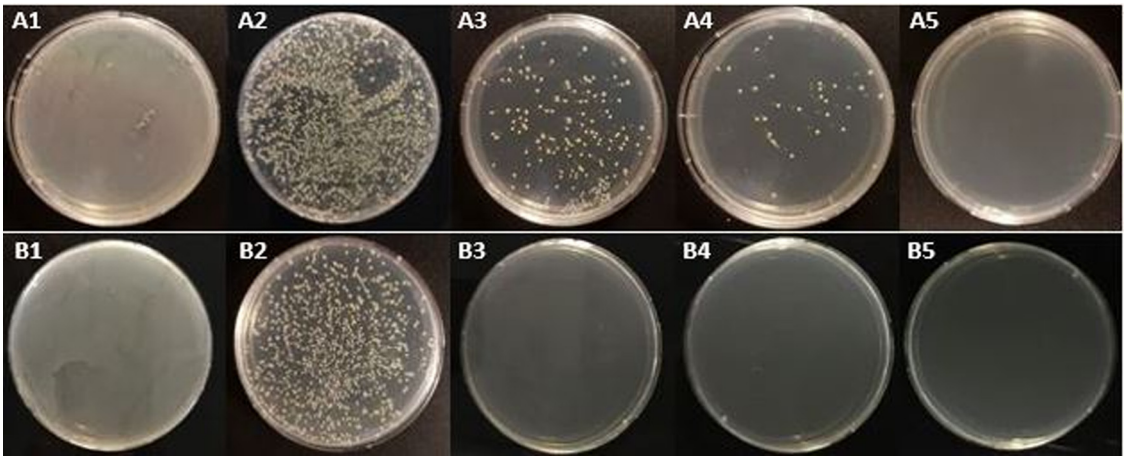

Figure 9: Growth of *S. aureus* (A) and *S. typhimurium* (B) on NA plates containing 0 (1) 30 (2), 60 (3), 100 (4), and 300 (5) µL of AgNP solution.

AgNP ions. In Gram-positive bacteria, such as *S. aureus*, the peptidoglycan layer as a protective coating is thicker when compared with that of Gram-negative bacteria. Furthermore, lipopolysaccharide with a negative charge can be another remarkable reason. The Gram-negative bacteria are coated with this molecule, which has a considerable affinity for NP ions. As a result, the growing uptake of ions leads to intracellular destruction. The findings in this article are in line with those of Jo et al. [40] and Priyanka Singh et al. [43], indicating that the synthesized AgNPs have a more destructive impact on Gram-negative than Gram-positive bacteria.

4 Concluding remarks

This study demonstrated an unsophisticated green synthesis of AgNPs, as a feasible alternative to the chemical as well as physical methods, by effectual bioreduction of Ag^+ using *C. vulgaris*, actively acting as reducing and stabilizing agents. With regard to the dried extract of *C. vulgaris*, various functional groups that existed in this extract are responsible for the synthesis. Instead of other time-consuming energy supplies, microwave irradiation was used as an abundant energy source. Mostly spherical NPs with size ranging from 1 to 50 nm and an average size of 24 nm could be monitored by SEM and TEM. Also, the distinctive inhibition effect of the formed NP against a variety of bacteria was represented. As future directions, another natural stabilizer beside *C. vulgaris* can be used to obtain AgNPs with higher stability. Due to the potential of *C. vulgaris* in being used as both reducing and stabilizing agents, the synthesis of other metal NPs can also be examined. There are other heating methods such as autoclave that can be assessed as an alternative energy supply to microwave irradiation to find out whether they work or not. Besides the considerable progress in nanobiotechnology, the more futuristic visions of nanoscience consist of the widespread use of NPs in biomedical and pharmaceutical applications.

Declaration

The abstract and preliminary results of this article were presented at the International Conference on Life and Engineering Sciences (ICOLES, July 2019), Istanbul Medipol University, Turkey.

Acknowledgments: The authors acknowledge Individual Research Funding (IRF) from the Sabanci University Nanotechnology Research and Application Centre (SUNUM). The authors thank PhD candidate Zeki Semih Pehlivan (SU) for the useful discussions.

References

[1] Manjunath HM, Joshi CG. Characterization, antioxidant and antimicrobial activity of silver nanoparticles synthesized using marine endophytic fungus-Cladosporium cladosporioides. Process Biochem. 2019;82:199–204.
[2] Pugazhendhi A, Prabakar D, Jacob JM, Karuppusamy I, Saratale RG. Synthesis and characterization of silver nanoparticles using Gelidium amansii and its antimicrobial property against various pathogenic bacteria. Microb Pathog. 2018;114:41–5.
[3] Shukla AK, Iravani S. Metallic nanoparticles: green synthesis and spectroscopic characterization. Environ Chem Lett. 2017;15:223–31.
[4] Saravanan M, Barik SK, MubarakAli D, Prakash P, Pugazhendhi A. Synthesis of silver nanoparticles from Bacillus brevis (NCIM 2533) and their antibacterial activity against pathogenic bacteria. Microb Pathog. 2018;116:221–6.
[5] Mandal AK. Silver nanoparticles as drug delivery vehicle against infections. Glob J Nanomed. 2017;3:1–4.
[6] Sri V, Pugazhendhi A, Gopalakrishnan K. Biofabrication and characterization of silver nanoparticles using aqueous extract of seaweed Enteromorpha compressa and its biomedical properties. Biotechnol Rep. 2017;14:1–7.
[7] Sreekanth T, Debbie CC. Metal nanoparticles: synthesis and applications in pharmaceutical sciences. Boschstr. 12, Weinheim, Germany: Wiley-VCH Verlag GmbH&Co. KGaA. 2018.
[8] Salmiati SA, Salim MR, Beng Hong Kueh A, Hadibarata T, Nur H. A review of silver nanoparticles: research trends, global consumption, synthesis, properties, and future challenges. J Chinese Chem Soc. 2017;64:732–56.
[9] Shankar S, Rhim JW. Preparation and characterization of agar/lignin/silver nanoparticles composite films with ultraviolet light barrier and antibacterial properties. Food Hydrocoll. 2017;71:76–84.
[10] Abdel-Raouf N, Al-Enazi NM, Ibraheem IBM, Alharbi RM, Alkhulaifi MM. Biosynthesis of silver nanoparticles by using of the marine brown alga Padina pavonica and their characterization. Saudi J Biol Sci. 2019;26:1207–15.
[11] Ahmed S, Annu, Ikram S, Yudha S. Biosynthesis of gold nanoparticles: a green approach. J Photochem Photobiol B Biol. 2016;161:141–53.
[12] Al-Bahrani R, Raman J, Lakshmanan H, Hassan AA, Sabaratnam V. Green synthesis of silver nanoparticles using tree oyster mushroom Pleurotus ostreatus and its inhibitory activity against pathogenic bacteria. Mater Lett. 2017;186:21–5.
[13] Costa S, Laryssa P, Pinto O, Jairo K, Wanderson JS Da, Romero AA, et al. Extracellular biosynthesis of silver nanoparticles using the cell-free filtrate of nematophagous

fungus Duddingtonia flagrans. Int J Nanomed. 2017;12:6373–81.
[14] Kim D, Saratale RG, Shinde S, Syed A, Ameen F, Ghodake G. Green synthesis of silver nanoparticles using *Laminaria japonica* extract: characterization and seedling growth assessment. J Clean Prod. 2018;172:2910–8.
[15] Neethu S, Midhun SJ, Radhakrishnan EK, Jyothis M. Green synthesized silver nanoparticles by marine endophytic fungus Penicillium polonicum and its antibacterial efficacy against biofilm forming, multidrug-resistant Acinetobacter baumannii. Microb Pathog. 2018;116:263–72.
[16] Mohanta Y, Nayak D, Biswas K, Singdevsachan S, Abd_Allah E, Hashem A, et al. Silver nanoparticles synthesized using wild mushroom show potential antimicrobial activities against food borne pathogens. Molecules. 2018;23:655.
[17] Hoseinnejad M, Jafari SM, Katouzian I. Inorganic and metal nanoparticles and their antimicrobial activity in food packaging applications. Crit Rev Microbiol. 2018;44:161–81.
[18] Torabfam M, Jafarizadeh MH. Microwave-enhanced silver nanoparticle synthesis using chitosan biopolymer: optimization of the process conditions and evaluation of their characteristics. Green Process Synth. 2018;7:530–7.
[19] Hussain I, Singh NB, Singh A, Singh H, Singh SC. Green synthesis of nanoparticles and its potential application. Biotechnol Lett. 2016;38:545–60.
[20] Parveen M, Ahmad F, Malla AM, Azaz S. Microwave-assisted green synthesis of silver nanoparticles from Fraxinus excelsior leaf extract and its antioxidant assay. Appl Nanosci. 2016;6:267–76.
[21] El-naggar ME, Shaheen TI, Fouda MMG, Hebeish AA. Eco-friendly microwave-assisted green and rapid synthesis of well-stabilized gold and core–shell silver–gold nanoparticles, Carbohydr Polym. 2016;136:1128–36.
[22] Palchik O, Zhu J, Gedanken A. Microwave assisted preparation of binary oxide nanoparticles. J Mater Chem. 2000;10:1251–4.
[23] Safi C, Zebib B, Merah O, Pontalier P-Y, Vaca-Garcia C. Morphology, composition, production, processing and applications of Chlorella vulgaris: a review. Renewable Sustainable Energy Rev. 2014;35:265–78.
[24] Přibyl P, Cepák V, Zachleder V. Production of lipids in 10 strains of Chlorella and Parachlorella, and enhanced lipid productivity in Chlorella vulgaris. Appl Microbiol Biotechnol. 2012;94:549–61.
[25] Rafique M, Sadaf I, Rafique MS, Tahir MB. A review on green synthesis of silver nanoparticles and their applications. Artif Cells Nanomedicine Biotechnol. 2017;45:1272–91.
[26] Alsammarraie FK, Wang W, Zhou P, Mustapha A, Lin M. Green synthesis of silver nanoparticles using turmeric extracts and investigation of their antibacterial activities. Colloids Surf B. 2018;171:398–405.
[27] Veisi H, Azizi S, Mohammadi P. Green synthesis of the silver nanoparticles mediated by Thymbra spicata extract and its application as a heterogeneous and recyclable nanocatalyst for catalytic reduction of a variety of dyes in water. J Clean Prod. 2018;170:1536–43.
[28] Raja S, Ramesh V, Thivaharan V. Green biosynthesis of silver nanoparticles using Calliandra haematocephala leaf extract, their antibacterial activity and hydrogen peroxide sensing capability. Arab J Chem. 2017;10:253–61.
[29] de Aragão AP, de Oliveira TM, Quelemes PV, Perfeito MLG, Araújo MC, Santiago J de AS, et al. Green synthesis of silver nanoparticles using the seaweed Gracilaria birdiae and their antibacterial activity. Arab J Chem. 2016:4182–8.
[30] Bagherzade G, Tavakoli MM, Namaei MH. Green synthesis of silver nanoparticles using aqueous extract of saffron (*Crocus sativus* L.) wastages and its antibacterial activity against six bacteria. Asian Pac J Trop Biomed. 2017;7:227–33.
[31] Arokiyaraj S, Vincent S, Saravanan M, Lee Y, Oh YK, Kim KH. Green synthesis of silver nanoparticles using Rheum palmatum root extract and their antibacterial activity against Staphylococcus aureus and Pseudomonas aeruginosa. Artif Cells Nanomed Biotechnol. 2017;45:372–9.
[32] Kasithevar M, Saravanan M, Prakash P, Kumar H, Ovais M, Barabadi H, et al. Green synthesis of silver nanoparticles using Alysicarpus monilifer leaf extract and its antibacterial activity against MRSA and CoNS isolates in HIV patients. J Interdiscip Nanomed. 2017;2:131–41.
[33] Francis S, Joseph S, Koshy EP, Mathew B. Microwave assisted green synthesis of silver nanoparticles using leaf extract of Elephantopus scaber and its environmental and biological applications. Artif Cells Nanomed Biotechnol. 2018;46:795–804.
[34] Rao B, Tang R-C. Green synthesis of silver nanoparticles with antibacterial activities using aqueous Eriobotrya japonica leaf extract. Adv Nat Sci Nanosci Nanotechnol. 2017;8:015014.
[35] Akther T, Mathipi V, Kumar NS, Davoodbasha M, Srinivasan H, Fungal-mediated synthesis of pharmaceutically active silver nanoparticles and anticancer property against A549 cells through apoptosis. Environ Sci Pollut Res. 2019;26:13649–57.
[36] Ghiuță I, Cristea D, Croitoru C, Kost J, Wenkert R, Vyrides I, et al. Characterization and antimicrobial activity of silver nanoparticles, biosynthesized using Bacillus species. Appl Surf Sci. 2018;438:66–73.
[37] Składanowski M, Wypij M, Laskowski D, Golińska P, Dahm H, Rai M. Silver and gold nanoparticles synthesized from *Streptomyces* sp. isolated from acid forest soil with special reference to its antibacterial activity against pathogens. J Clust Sci. 2017;28:59–79.
[38] AbdelRahim K, Mahmoud SY, Ali AM, Almaary KS, Mustafa AE-ZMA, Husseiny SM. Extracellular biosynthesis of silver nanoparticles using Rhizopus stolonifer. Saudi J Biol Sci. 2017;24:208–16.
[39] Wang C, Kim YJ, Singh P, Mathiyalagan R, Jin Y, Yang DC. Green synthesis of silver nanoparticles by *Bacillus methylotrophicus*, and their antimicrobial activity. Artif Cells Nanomed Biotechnol. 2016;44:1127–32.
[40] Jo JH, Singh P, Kim YJ, Wang C, Mathiyalagan R, Jin CG, et al. Pseudomonas deceptionensis DC5-mediated synthesis of extracellular silver nanoparticles. Artif Cells Nanomed Biotechnol. 2016;44:1576–81.
[41] Singh P, Kim YJ, Wang C, Mathiyalagan R, Yang DC. Weissella oryzae DC6-facilitated green synthesis of silver nanoparticles and their antimicrobial potential. Artif Cells Nanomed Biotechnol. 2016;44:1569–75.
[42] Wang L, He D, Gao S, Wang D, Xue B, Yokoyama K. Biosynthesis of silver nanoparticles by the fungus *Arthroderma fulvum* and its antifungal activity against genera of *Candida*, *Aspergillus* and *Fusarium*. Int J Nanomed. 2016;11:1899.

[43] Singh P, Kim YJ, Singh H, Mathiyalagan R, Wang C, Yang DC. Biosynthesis of anisotropic silver nanoparticles by Bhargavaea indica and their synergistic effect with antibiotics against pathogenic microorganisms. J Nanomater. 2015;2015:1–10.

[44] Elbeshehy EKF, Elazzazy AM, Aggelis G. Silver nanoparticles synthesis mediated by new isolates of *Bacillus* spp., nanoparticle characterization and their activity against bean yellow mosaic virus and human pathogens. Front Microbiol. 2015;6:1–13.

[45] Soni N, Prakash S. Antimicrobial and mosquitocidal activity of microbial synthesized silver nanoparticles. Parasitol Res. 2015;114:1023–30.

[46] Waghmare SR, Mulla MN, Marathe SR, Sonawane KD. Ecofriendly production of silver nanoparticles using Candida utilis and its mechanistic action against pathogenic microorganisms. 3 Biotech. 2015;5:33–8.

[47] Kathiraven T, Sundaramanickam A, Shanmugam N, Balasubramanian T. Green synthesis of silver nanoparticles using marine algae Caulerpa racemosa and their antibacterial activity against some human pathogens. Appl Nanosci. 2015;5:499–504.

[48] Mahajan A, Arya A, Chundawat TS. Green synthesis of silver nanoparticles using green alga (*Chlorella vulgaris*) and its application for synthesis of quinolines derivatives. Synth Commun. 2019;49:1926–37.

[49] (Yalcin) Duygu D. Fourier transform infrared (FTIR) spectroscopy for identification of Chlorella vulgaris Beijerinck 1890 and Scenedesmus obliquus (Turpin) Kützing 1833. Afr J Biotechnol. 2012;11:3817–24.

[50] Slavin YN, Asnis J, Häfeli UO, Bach H. Metal nanoparticles: understanding the mechanisms behind antibacterial activity. J Nanobiotechnol. 2017;15:1–20.